Journal of Basic and Applied Research International
3(3): 94-101, 2015

International Knowledge Press
www.ikpress.org

ELECTRICAL ANISOTROPY CHARACTERIZATION OF FRACTURED CRYSTALLINE BASEMENT ROCK AT IGARRA, NIGERIA

I. I. OBIADI[1*], A. G. ONWUEMESI[1], O. L. ANIKE[1], C. M. OBIADI[1], N. E. AJAEGWU[1], E. K. ANAKWUBA[1], V. U. MADUEWESI[1] AND E. O. EZIM[1]
[1]Department of Geological Sciences, Nnamdi Azikiwe University, Awka, Nigeria.

AUTHORS' CONTRIBUTIONS
This work was carried out in collaboration between all authors. All authors read and approved the final manuscript.

Received: 9th December 2014
Accepted: 9th January 2015
Published: 17th February 2015

Research Article

ABSTRACT

Electrical anisotropy, which refers to the variation of electrical resistivity (or conductivity) with direction, is exhibited by most rocks. In crystalline rocks, electrical anisotropy may result from the preferred orientation of mineral crystal (banding and foliation), cracks, fractures and cleavages which are products of pressure and dynamic processes. Surface geological and geophysical surveys were done at locations within the study area, with the aim of identifying and characterizing electrical anisotropy within the crystalline basement rocks at Igarra. Electrical anisotropy was quantified from the geophysical data by the use of anisotropic parameters of Percentage of Anisotropy, Apparent Anisotropy and Coefficient of Anisotropy. All three parameters showed that electrical anisotropy increases with depth while inhomogeneity is maximum at shallow depth. Analysis and correlation of the surface geological and geophysical data showed that the major cause of electrical anisotropy is the presence of fractures in the rock mass. These fractures which have dominant strike orientation in the N-S direction causes a significant decrease in apparent resistivity in the orientation parallel to its strike and a corresponding increase in apparent resistivity in the direction perpendicular to its strike direction. The increase in electrical anisotropy with depth suggests that the intensity of fracturing (fracture density) increases with depth.

Keywords: Electrical anisotropy, fractures, electrical resistivity, crystalline rocks.

1. INTRODUCTION

Electrical anisotropy, which refers to the variation of electrical resistivity (or conductivity) with direction, is exhibited by most rocks. In crystalline rocks, electrical anisotropy may result from the preferred orientation of mineral crystals (banding and foliation), cracks, fractures and cleavages which are products of pressure and dynamic processes [1]. In sediments and sedimentary rocks, anisotropy is caused by the gravity-induced alignment of elongated or flattened grains parallel to the bedding planes. In case of prolate anisotropy, the longitudinal resistivity ℓ_L parallel to this preferred anisotropy plane is less than the transverse resistivity ℓ_T, which is perpendicular to this plane. For a given geologic model:

**Corresponding author: Email: izuchukwuig@yahoo.com;*

$$\lambda = \sqrt{(\ell_T / \ell_L)} \quad (1)$$

and

$$\ell_m = \sqrt{(\ell_L \times \ell_T)} \quad (2)$$

where λ is the coefficient of anisotropy and ℓ_m is the mean apparent resistivity. This paper presents a case study on the characterization of electrical anisotropy in fractured crystalline basement rock at Igarra, Nigeria using the Square Array Electrical Resistivity method.

All resistivity methods employ the use of artificial source of current (DC or low frequency AC), which is introduced into the ground through point metallic stake (electrode) or long line contact. The purpose of resistivity survey is to determine the subsurface resistivity distribution by making measurement on the ground surface. The ground resistivity is related to various geologic parameters such as the fluid and mineral content, and alignment; porosity, degree of water saturation, temperature and geologic structures such as fractures, foliation or banding [1]. The fundamental physical law used in resistivity survey is the Ohm's law that governs the flow of current in the ground. The equation of Ohm' law in the vector form for current flow in a continuous medium is given by

$$\mathbf{J} = \boldsymbol{\sigma}\mathbf{E} \quad (3)$$

Where **J** is the current density, $\boldsymbol{\sigma}$ is the conductivity of the medium and **E** is the electric field.

The square array configuration employs the use of four electrodes – two current electrodes and two potential electrodes arranged at the corners of a square of size 'a'. Measurements are recorded at the center of the square. To estimate the variation of apparent resistivity with depth, the array is symmetrically expanded about its center in simple multiples (Fig. 1), while to obtain apparent resistivity measurements along different azimuths, complete expansions are rotated at regular angular increments through 180° (Fig. 2). The orientation of the azimuth of measurement is the line between the two current electrodes. Plots of the apparent resistivity values as a function of azimuth are used to characterize electrical anisotropy. When the data are plotted in the polar coordinate, circular plots are characteristically interpreted to indicate electrical isotropy, signifying the absence of measurable fracture set of preferred orientation or small volume of rock investigated [2]. On the other hand, elliptical plots are generally construed to signify anisotropic response within the rock mass.

2. REGIONAL GEOLOGY AND TECTONICS OF STUDY AREA

Lithologically, Igarra comprises mainly the slightly Migmatised to Unmigmatised Schist Belt (Igarra Schist Belt) bounded and underlain by the Migmatite – Gneiss Complex and intruded by the Pan-African Older Granite which forms good topographic features rising up to over 100 m above the surrounding terrains (Fig. 3). The contact between the Migmatite-Quartzite Complex and the Schist Belt are sometimes fault bounded. The Igarra Schist runs for about 60km in a generally NNW – SSE direction [3] and comprises Quartz-Biotite Schist, Mica Schist, Quartzite and Quartz Schist, Calc-Silicate and Marble; and Metaconglomerate.

The Quartz-Biotite Schist is the dominant rock type in the area. The rock is dark coloured with narrow alternating dark and light grey bands. The dark bands are composed mainly of biotite and garnet while the light grey bands comprise mainly quartz, feldspar and epidote. Either band can increase in thickness at the expense of the other such that the rock can locally assume gneissic or schistose texture. The unit has been migmatised and granitised in some places as a result of emplacement of the Pan-African granites.

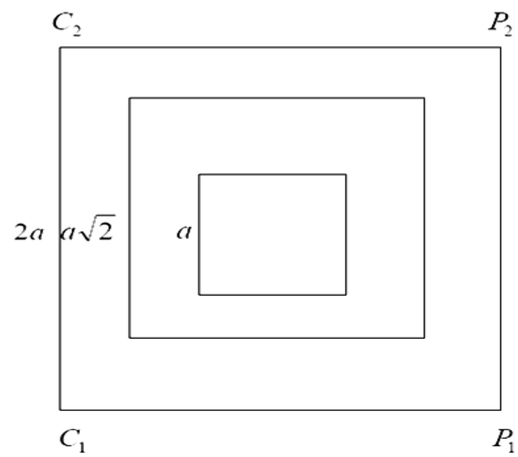

Fig. 1. Symmetrical expansion of the square array about its centre

The Mica-Schist is mainly medium to coarse grained within which bands of quartzite occur. The inter-layering has been attributed to both metamorphic recrystallization and a rhythmic transgressive and regressive inter-layering of facies.

The Metaconglomerate is made up of polymictic pebble, cobbles and boulder of calc-silicate gneiss, quartzite, marble, quartz-biotite schist as well as granite gneiss.

The Schist Belt is of the Upper Greenschist facies, and is believed to be relics of a supercrustal cover which was infolded into the Migmatite-Gneiss Complex [4]. Several workers have proposed models for the tectonic evolution of the Schist Belt in relation to the basement Complex. Ajibade [5] suggested an initial crustal extension and continental rifting at the West African craton margin about 1000 ma leading to the formation of graben-like structures in Western Nigerian and the subsequent deposition of the rocks of the Schist Belt. Closure of the ocean at the cratonic margin about 600 ma and crustal thickening in the Dahomeyan led to the deformation of the sediment, the reactivation of pre-existing rocks and the emplacement of the Pan-African granites. Recognition of suture along the eastern margin of the West African craton led Turner [6] to relate the Schist Belt to the subduction processes in the cratonic margin. He is of the view that the schist belt was deposited in a back-arc basin developed after the onset of subduction at the cratonic margin. However, the distance of the nearest Nigerian Schist Belt from the site of subduction is at least 200-250 km exceeding the 100-150 km from arc to back-arc basins in present day arc system [7]. The possibility that the Schist Belt may represent additional micro-continents separating pre-existing macro-continents have also been suggesting by McCurry and Wright [8].

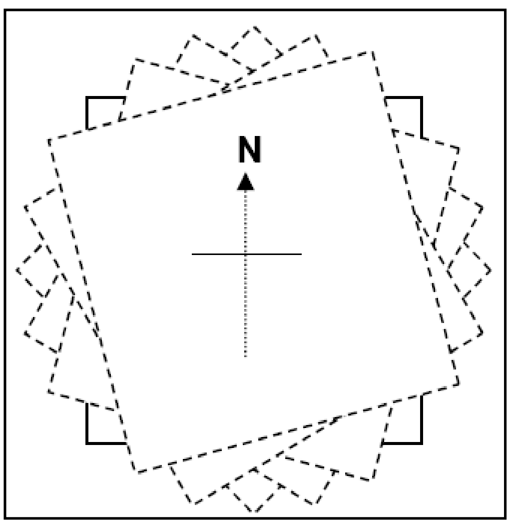

Fig. 2. Rotation of the square array at increments of 15°

3. METHODOLOGY

Surface geological mapping was first done at outcrops in the area with the aim of studying the rocks and geologic structures as well as the attitude of the mapped structures. Rock type and geologic structures (both primary and secondary structures) are some of the factors that influence the electrical properties of rocks (Fig. 4). This was followed by geophysical surveys done at two carefully selected sites. These sites are locations of minimal topographic undulation because topographic variations causes artificial terrain induced conductive and resistive anomalies in the field [10]. The method used for the geophysical survey is the Square Array Resistivity method. The survey is conducted by arranging four electrodes (two potential and two current) at the four corners of a square of side ‘a’. The value of ‘a’ which is the electrode spacing is directly related to the depth of investigation. According to Edwards [11], the estimated depth of investigation of the square array is 0.451 times the electrode spacing/sides of the square (a). The minimum and maximum electrode spacing used for this survey is 5 m and 40m respectively, corresponding to depth of investigation ranging from 2.3 to 18 m. The minimum spacing value was progressively increased by the factor a√2 (Fig. 1). To measure the directional variations of resistivity with azimuth, which is a measure of electrical anisotropy, initial array orientation was aligned in the direction of true north, and subsequent measurements along other azimuths were taken by progressively rotating the square about its center at angular increment of 22.5° through 157.5°. Readings were also taken in orientations perpendicular and parallel to the dominant fracture strike in the area because fractures are major causes of electrical anisotropy in crystalline rocks [12]. The Resistivity Earth Model 500 was used for taking resistivity measurement.

This survey design was done for all electrode spacing and at all two site locations investigated; and reading documented.

4. DATA ANALYSIS AND RESULTS

The surface geophysical data obtained from the field survey were analyzed and quantified for electrical anisotropy with the use of the following electrical anisotropy measures.

4.1 Percentage of Anisotropy

This was computed using the relations proposed by Busby [13]. The relation, known as the variation about the measurement average recorded is given by:

$$\pm 0.5\left(\frac{\ell_{\max}-\ell_{min}}{\ell_{avarage}}\right)100\% \qquad (4)$$

Where ℓ_{max}, ℓ_{min} and $\ell_{average}$ are maximum, minimum and average apparent resistivity values respectively, measured at a given location for a given 'a' spacing. Comparing the values of this ratio at different electrode spacing can be used to determine the percentage of anisotropy in the study area. The computed percentage of anisotropy value for the two site locations A and B are presented in Tables 1 and 2 respectively and their plots presented in Fig. 5.

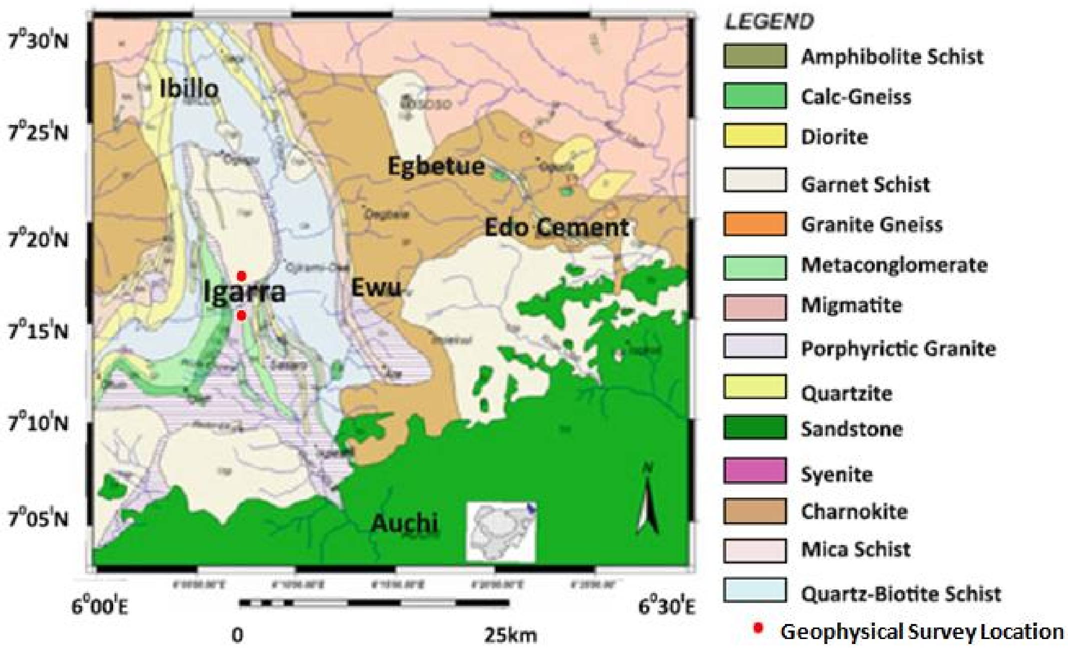

Fig. 3. Geologic map of Igarra area showing geophysical survey point locations (modified from [9])

Fig. 4. Exposed schist along River Ole Bank showing light coloured bands

4.2 Apparent Anisotropy (λ_a)

The apparent anisotropy (λ_a) was computed using the following relation:

$$\lambda_a = \frac{\ell_T}{\ell_L} = \frac{N(\sqrt{(N2+1)}-1)}{(\sqrt{(N2+1)}-N)} \qquad (5)[14]$$

Where ℓ_L and ℓ_T are apparent resistivity parallel to dominant fracture strike and apparent resistivity perpendicular to dominant fracture strike as determined from the surface geologic and geophysical surveys; and N is effective vertical anisotropy. Computed values of apparent anisotropy are presented in Tables 3 and 4 while the plot is presented in Fig. 6.

4.3 Coefficient of Anisotropy

A similar measure of anisotropy, the coefficient of anisotropy (λ) was computed also. It is defined by:

$$\lambda = \sqrt{\frac{\ell_T}{\ell_L}} \qquad (6)\ [15]$$

Table 1. Computed values of percentage of anisotropy at Anglican Science College, Igarra

a(m)	$\ell_{average}$	ℓ_{max}	ℓ_{min}	% anisotropy
5	172.3	198	170	8.125
7.1	130	170	125	17.308
10	113.2	150	110	17.668
14.1	105.5	150	110	18.957
20	123.5	175	125	20.243
28.3	149.4	230	120	36.814
40	188.3	320	200	31.864

Table 2. Computed values of percentage of anisotropy at Technical and Science College, Igarra

a(m)	$\ell_{average}$	ℓ_{max}	ℓ_{min}	% anisotropy
5	266.2	370	310	11.27
7.1	150.2	210	150	19.973
10	107.4	190	115	34.916
14.1	106.9	185	155	14.032
20	125	245	150	38
28.3	139	300	150	53.957
40	193.8	340	235	27.09

Values of the coefficient of anisotropy can be used to estimate in quantitative measures the change in resistivity over two perpendicular orientations within the rock mass (electrical anisotropy). For a homogeneous, isotropic surface resistivity measured in any given direction will be equivalent, i.e. ℓ_T will be equal to ℓ_L resulting in a value of 1 for λ. However, for anisotropic media, ℓ_T is not equal to ℓ_L giving rise to λ with value $\neq$ 1. According to Kunetz [16], λ values typically ranges between 1 and 2 since ℓ_T is usually greater than ℓ_L (prolate anisotropy). However, anthracite coal and graphite slate by Keller and Frishknecht [15] gave values greater than 2. Computed values of coefficient of anisotropy are presented in Tables 5 and 6 while the plot is presented in Fig. 7.

Table 3. Computed values of apparent anisotropy at Anglican Science College, Igarra

a(m)	ℓ_T	ℓ_L	λ_a
5	198	170	1.165
7.1	170	125	1.36
10	150	110	1.364
14.1	150	110	1.364
20	175	125	1.4
28.3	230	120	1.917
40	320	200	1.6

Table 4. Computed values of apparent anisotropy at Technical and Science College, Igarra

a(m)	ℓ_T	ℓ_L	λ_a
5	370	310	1.194
7.1	210	150	1.4
10	190	115	1.652
14.1	185	155	1.194
20	245	150	1.633
28.3	300	150	2
40	340	235	1.447

Table 5. Computed values of coefficient of anisotropy at Anglican Science College, Igarra

a(m)	ℓ_T	ℓ_L	λ
5	198	170	1.079
7.1	170	125	1.166
10	150	110	1.168
14.1	150	110	1.168
20	175	125	1.183
28.3	230	120	1.384
40	320	200	1.265

5. RESULT INTERPRETATION AND DISCUSSION

Data collected from Azimuthal Square Array Resistivity survey showed significant variation of apparent resistivity for different azimuthal array orientations at the two site locations investigated. Variation of apparent resistivity with azimuth result when the rock mass is anisotropic and/or inhomogeneous. Anisotropy may result, generally from the presence of fractures and/or preferential alignment of minerals or foliations in the rock mass. Anisotropy can also result from other depositional processes. However, fracturing remains a major cause of anisotropy in rocks [12]. Electrical anisotropy in the study area was characterized by the use of three anisotropic measures. The percentage anisotropy distinguishes anisotropy from inhomogeneity [13]. Computed values of percentage anisotropy (Tables 1 and 2) showed that at small electrode spacing corresponding to shallow or near surface depth, electrical anisotropy is relatively small, while with increase in depth represented by subsequent increase in electrode spacing, electrical anisotropy increases (Fig. 5). The relative increase in the value of coefficient of anisotropy with depth supports the inferences from the result of the computed values of percentage of anisotropy. According to Kunetz [16], the value of the coefficient of anisotropy varies from 1 – 2. At relatively shallow depth, the value of the coefficient of anisotropy approaches unity suggesting inhomogeneity with little anisotropic effect, but with depth there is a general increase in the value of the coefficient of anisotropy indicating more anisotropic effects with depth relative to inhomogeneity. The relative high inhomogeneity at shallow depth is likely attributed to the effect of weathering as observed from the surface geologic field mapping. Large boulders of quartz which is relatively resistant to weathering are observed scattered within the shallow depth zone in the study area. These quartz boulders together with the weathered products from the crystalline rock at shallow depth results in inhomogeneity at the shallow zone. This same observation of increase in electrical anisotropy with depth was also observed for the computed values of apparent anisotropy. These in-situ electrical anisotropy parameter measures are mainly attributed to fractures in the crystalline basement rock since apparent resistivity values measured in the field generally decreases in the orientation parallel to the dominant fracture strike and increases in the orientation perpendicular to the dominant fracture strike. Analysis of the surface geologic field data showed that the dominant fracture strike orientation is in the N-S direction (Fig. 8).

Table 6. Computed values of coefficient of anisotropy at Technical and Science College, Igarra

a(m)	ℓ_T	ℓ_L	λ
5	370	310	1.092
7.1	210	150	1.183
10	190	115	1.285
14.1	185	155	1.092
20	245	150	1.278
28.3	300	150	1.414
40	340	235	1.203

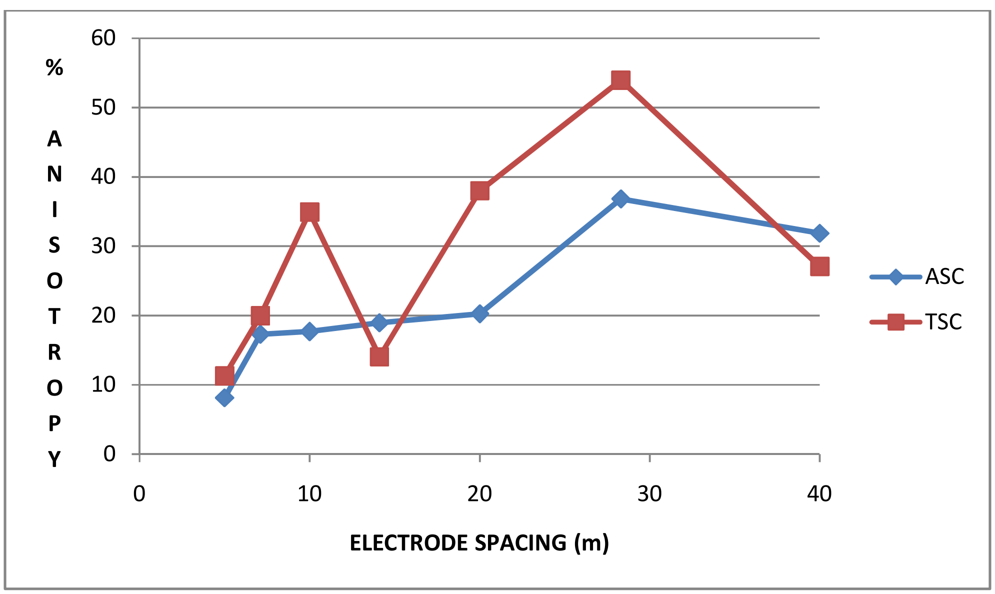

Fig. 5. Plot of percentage anisotropy versus electrode spacing for surveys done at Anglican Science College (ASC) and Technical Science College (TSC)

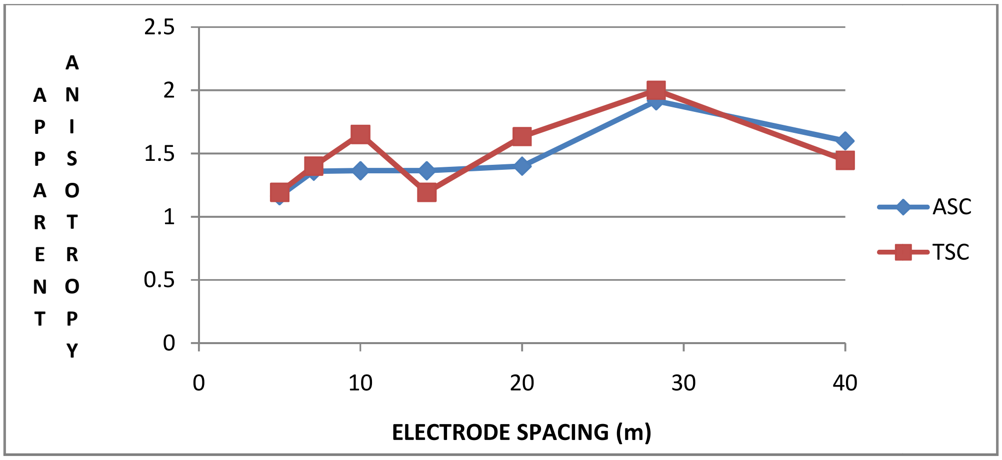

Fig. 6. Plot of apparent anisotropy versus electrode spacing for surveys done at Anglican Science College (ASC) and Technical Science College (TSC)

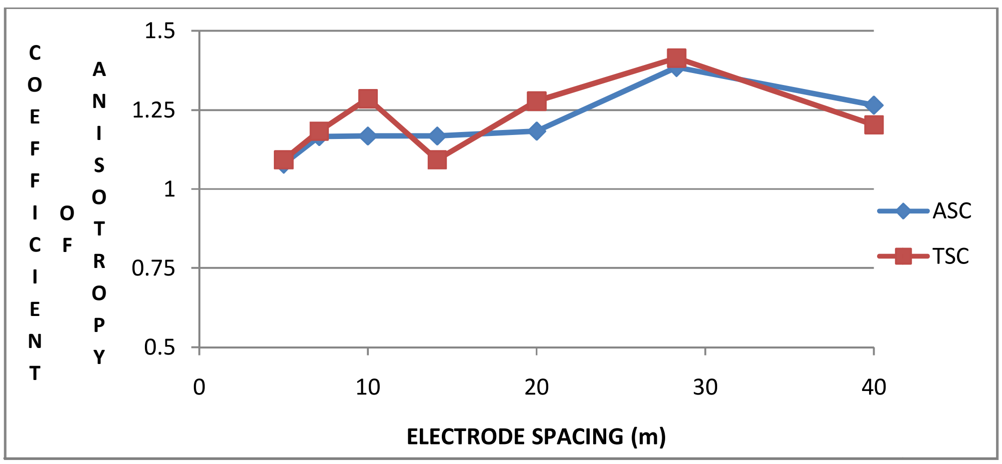

Fig. 7. Plot of coefficient of anisotropy versus electrode spacing for surveys done at Anglican Science College (ASC) and Technical Science College (TSC)

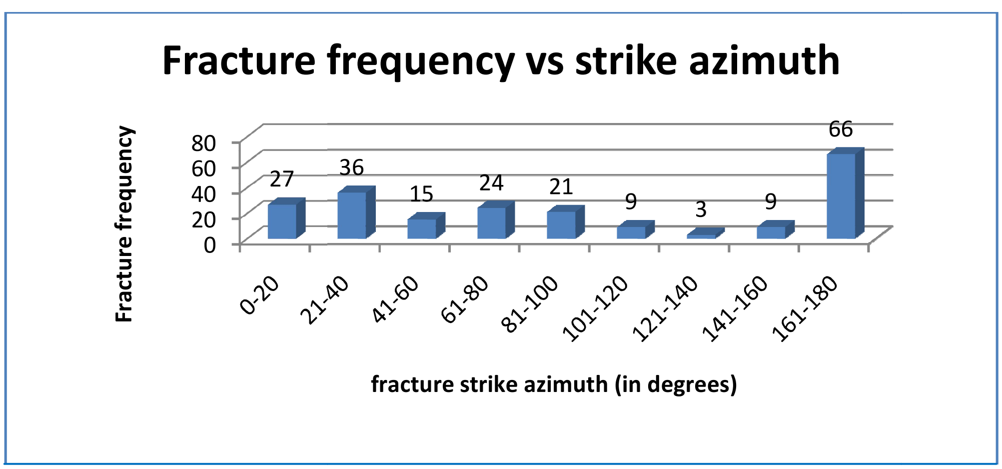

Fig. 8. Plot of fracture frequency against fracture azimuth for fracture data obtained from surface geological field mapping

6. CONCLUSION

Most rocks exhibit electrical anisotropy, the variation of resistivity (or conductivity) with direction. In crystalline rocks, anisotropy may arise from preferred orientation of mineral crystals, cracks and fractures, and cleavages as a result of pressure and dynamic processes. Fractures contribute greatly to electrical anisotropy, creating zones of contrasting electrical properties in the bedrock – increasing electrical conductivity along the direction of the fracture strike while decreasing same in the direction perpendicular to fracture strike. Surface geologic and geophysical surveys were done to identify and characterize electrical anisotropy at Igarra, Nigeria. Electrical anisotropy was quantified using anisotropic parameters of percentage of anisotropy, apparent anisotropy and coefficient of anisotropy. All these parameters showed that electrical anisotropy increases with depth while inhomogeneity is maximum close to the surface/shallow depth. The major cause of electrical anisotropy in the study area is the presence of fractures in the rock mass. These fractures which have dominant strike orientation in the N-S direction cause a significant decrease in apparent resistivity in that orientation and a significant increase in apparent resistivity in the direction perpendicular to the dominant fracture strike orientation. And since electrical anisotropy increases with depth, it therefore suggests that the intensity of fracturing (fracture density) increases with depth.

COMPETING INTERESTS

Authors have declared that no competing interests exist.

REFERENCES

1. Hagrey SA. Electric study of fracture anisotropy at Falkenberg, Germany. Geophysics. 1994;(59):881-888.
2. Busby JP, Peart PJ. Azimuthal resistivity and seismic measurements for the determination of fracture orientations. Geological Society, London, Engineering Geology Special Publications. 1997;(12):273-281.
3. Rahaman MA. A review of the basement geology of south-western Nigeria. In Kogba, C.A. (ed), Geology of Nigeria, Elizabethan Publ. Co., Lagos. 1976;41-58.
4. McCurry P. Geology of degree sheet (Zaria). Overseas Geol. Min. Res. 1973;45
5. Ajibade AC. Geotectonic evolution of the Zungeru Region, Nigeria. Unpublished P.hD thesis, University of Wales, UK; 1980.
6. Turner DC. Upper Proterozoic schist belt in the Nigerian sector of the Pan-African province of West Africa. Precambrian Research. 1983;(21):55-75.
7. Gass IG. Pan-African (Upper Proterozoic) plate tectonics of the Arabian-Nubian shield. In Kroner A. (ed), Precambrian Plate Tectonics, Elsevier, Amsterdam. 1981;387-402.
8. McCurry P, Wright JB. Geochemistry of calc-alkaline volcanic in northwestern Nigeria and a possible Pan-African suture zone. Earth Planet. Sci. Lett. 1977;(37):90-96.
9. Anifowose AYB, Bamisaye OA, Odeyemi IB. Establishing a solid mineral database for part of Southwestern Nigeria, Geospatial World Newsletter; 2006. Available:www.geospatialworld.net
10. Telford WM, Geldart LP, Sheriff RE. Applied Geophysics (Second edition) Cambridge University Press, Cambridge. 1990;770.
11. Edwards LS. A modified pseudosection for resistivity and IP. Geophysics. 1977;(42):1020-1036.
12. Anderson B, Bryant I, Luling M, Spies B, Helbig K. Oilfield anisotropy: Its origins and electrical characteristics. Oilfield Review. 1994;(6):48-56.
13. Busby JP. The effectiveness of azimuthal apparent-resistivity measurements as a method for determining fracture strike orientations. Geophysical Prospecting. 2000;(48):677–695.
14. Darboux-Afouda R, Louis P. Contribution measurements of anisotropic crystalline electric research environment fractured aquifers in Benin. Geophysical Prospecting. 1989;(37):91-105.
15. Keller GV, Frischknecht FC. Electrical methods in geophysical prospecting. Pergamon Press, New York. 1966;519.
16. Kunetz G. Principles of direct current resistivity prospecting. Gebriider Borntraeger, Berlin. 1966;103.